NUMERICAL MODELLING AND EXPERIMENTAL VERIFICATION OF GLASS–POLYESTER MIXED LAMINATE BEAM BENDING TEST

Agnieszka BONDYRA[*], Marian KLASZTORNY[*], Piotr SZURGOTT[*], Paweł GOTOWICKI[*]

[*]Department of Mechanics and Applied Computer Science, Faculty of Mechanical Engineering, Military University of Technology, ul. Gen. S. Kaliskiego 2, 00-908 Warszawa, Poland

abondyra@wat.edu.pl, mklasztorny@wat.edu.pl, pszurgott@wat.edu.pl, pgotowicki@wat.edu.pl

Abstract: The subject undertaken in the study is a glass (fibre) – polyester (matrix) layered composite, of the mixed sequence, composed alternately of laminas reinforced with E-glass plain weave fabric (WR600) and E-glass mat (CSM450). The laminate is manufactured on Polimal 104 polyester matrix. The aim of the study is to determine the options/values of parameters for numerical modelling and simulation of static processes in shell structures made of glass-polyester composites undertaken, in MSC.Marc system, recommended in engineering calculations. The effective elastic and strength constants of homogeneous laminas have been determined experimentally according to the standard procedures. The bending test of composite beams has been conducted experimentally and simulated numerically. Numerical investigations have been focused on selection of options/values of the numerical modelling and simulation parameters. The experimental verification of numerical modelling of the bending test is positive in both the quasi-linear range and in the catastrophic – progressive failure zone.

Key words: GRRP Shells, Beam Bending Test, FEM Numerical Modelling, Experimental Verification

1. INTRODUCTION

Wide practical applications of layered polymer-matrix composites first of all result from high relative strength and high relative stiffness of these materials which also exhibit high environmental and chemical resistance. Composite covers of tanks and canals, including wastewater purification plants, are one of the most important areas of practical applications of glass–polyester laminates (see product catalogues of Meier, 2006; Glaplast, 2010).

Numerical modelling and simulation of polymer-matrix composite structures using commercial CAE systems is at early stage of research and development. CAE systems, e.g. MSC.Marc (2008a, 2008b, 2008c) or LS-Dyna (2009), indicate wide possibilities for laminates modelling but, up-to-date, scientists have not developed sets of options/values of parameters recommended in engineering calculations for numerical modelling and simulation of static, rheological, dynamic or impact processes. Special attention should be put onto laminates which exhibit multiple modes of damage and fracture due to their heterogeneity and microstructure.

In problem-oriented references, one can find contributions which develop numerical modelling of polymer-matrix composite structural elements, but the data and descriptions incorporated in those papers are not satisfactory. For example, Vacĭk et al., (2010) presented numerical modelling of the three-point bending test of composite beams using MSC.Marc system. The considerations have been limited to adequacy assessment of various FE types and their combinations (Element_149, Element_22 i Element_75 among the others). Part of the contribution by Zemčĭk et al., (2011) is devoted to numerical analysis of the bending tests for laminates reinforced with glass mat and glass fabric. Modelling methodology description has been limited to giving the material constants, the failure criterion (Hashin) and the residual stiffness factor.

FEM numerical modelling, engineering calculations and design of composite covers of engineering structures is a topical theme in civil engineering. The reasons are collected below:

- a large quantity of serviced composite covers;
- a large quantity of tanks, pools, canals, objects in wastewater treatment plants, and other objects which require composite covers;
- a large quantity of geometric, material, and structural solutions in reference to composite covers;
- no standards and engineering handbooks for design of composite covers and demand for such contributions in design offices;
- rare catastrophic failures of composite covers especially in winter conditions;
- potential military applications of composite covers.

The study develops numerical modelling and experimental verification related to the bending test of beams made of mixed glass–polyester layered composite applied for manufacturing of shell segments for the Klimzowiec wastewater purification plant. The structural material has a mixed symmetric stacking sequence and is manufactured using the contact technology.

The general concept of this study is presented below. The effective elastic and strength constants of uniform laminas have been determined experimentally according to standards PN-EN ISO (1997, 2000, 2001b, 2002) and ASTM (1998). The composite beam bending test has been executed experimentally according to the standard procedure. FEM numerical modelling related to the static bending test of the mixed laminate beam has been developed using FE code MSC.Marc/Mentat. The numerical research has been focussed on selection of options/values of the numerical modelling and simulation parameters. The simulation results have been compared to the respective experimental results (verification). Finally, a set of options/values of numerical modelling and simulation parameters in reference to static pro-

cesses up to total failure in glass–polyester laminate shell structures has been proposed. This set, corresponding to FE code MSC.Marc, is recommended in engineering calculations.

2. DESCRIPTION OF THE COMPOSITE AND EXPERIMENTAL BENDING TEST

The subject of the research is a mixed GFRP structural laminate, denoted with MT code, manufactured using the following components: Polimal 104 polyester resin as the matrix (produced by Organika-Sarzyna Co., Poland), CSM450 E-glass mat and WRF600 E-glass fabric as reinforcement (produced by Krosglass Co., Poland). The laminate has the following stacking sequence: [(CSM450/WRF600)$_3$/CSM450]. WRF600 two-directional balanced plain weave fabric is characterized by 600 g/m^2 G.S.M. and orientation [0/90] with respect to the beam principal axes. The MT laminate has thickness h = 6.1 mm (the average value) and the average thicknesses of laminas are 1.0/0.7/1.0/ 0.7/1.0/0.7/1.0 mm, respectively.

Uniform laminas are denoted as M (mat reinforcement) and T (fabric reinforcement). In order to determine the effective material constants of uniform laminas, the following uniform plate semi-finished products have been manufactured: M (5CSM450) and T (4WR600). The plate semi-finished products MT, M, and T, of overall dimensions 500×500 mm, have been manufactured in ROMA Ltd., Grabowiec, Poland, using the contact technology with technological parameters compatible with the Polimal 104 resin card (2008). This card points out the following properties: good processing properties, good wettability of glass fibre, high strength parameters, good resistance to atmospheric factors.

The effective material constants of uniform laminas, i.e. M lamina reinforced with CSM450 E-glass mat and T lamina reinforced with WRF600 E-glass fabric, have been derived experimentally using respective standard specimens. In the modelling, the average values of those constants have been applied. The following standard tests have been examined:

– in–plane unidirectional static compression according to PN-EN ISO 14126:2002 standard;
– out–of–plane static shear according to PN-EN ISO 14130:2001 standard;
– in–plane unidirectional static tension according to PN-EN ISO 527:2000 standard;
– in–plane static shear according to PN-EN ISO 14129:1997 and ASTM D5379 / D5379M - 98 standards.

The principal directions of M, T, and MT composites are denoted as 1, 2, 3, with the 1-2 lamina plane.

The in–plane unidirectional static compression test, according to PN-EN ISO 14126:2002, enables determining the following constants: X_c – compressive strength in direction 1, e_{1c} – ultimate normal strain at compression in direction 1, E_{1c}– Young's modulus at compression in direction 1, ν_{12c} – Poisson's ratio at compression in direction 1 in the 1-2 plane, ν_{13c} – Poisson's ratio at compression in direction 1 in the 1-3 plane.

PN-EN ISO 14130:2001 standard determines the nominal interlaminar shear strength S_{13}. For this test one can calculate approximately shear strain γ_{13} close to the beam horizontal central plane based on the deflection of the short beam (with dominant shear) and calculate the following constants: G_{13} – shear modulus in the 1-3 plane, g_{13} – ultimate shear strain in the 1-3 plane.

The in–plane unidirectional static tension test, according to PN-EN ISO 527:2000, enables determining the following constants: X_t – tensile strength in direction 1, e_{1t} – ultimate normal strain at tension in direction 1, E_{1t} – Young's modulus at tension in direction 1, ν_{12t} – Poisson's ratio at tension in direction 1 in the 1-2 plane.

The in–plane static shear test for T laminate is performed by tension at angle ±45° in reference to principal direction 1 (PN-EN ISO 14129:1997), whereas for M laminates Iosipescu method is applied (ASTM D5379 / D5379M - 98). The following material constants are determined: S_{12} – in-plane shear strength, G_{12} – in-plane shear modulus, g_{12} – ultimate shear strain in the 1-2 plane.

In addition, non-standard unidirectional compression test in direction 3 has been performed in order to derive the following constants: Z_c – out-of-plane compressive strength, e_{3c} – ultimate normal strain at compression in direction 3, E_{3c} – Young's modulus at compression in direction 3. In this test requirements related to the in–plane unidirectional static compression were followed. Specimens used in the out-of- plane compression test were shaped via sticky of three 10×10 mm plates of M or T type.

The examined specimens of dimensions, dimensional tolerances and final processing determined in standards PN-EN ISO (1997, 2000, 2001b, 2002) were conditioned over 88 hours at 23±2°C temperature and 50±10% relative humidity. The experiments were performed at the same atmospheric conditions.

Independently of the identification tests performed on M and T uniform laminates, the standard tensile test for Polimal 104 polyester resin plastic has been done. The matrix was modelled as isotropic and linear elastic–short material, described by the classic constants: E – Young's modulus, ν – Poisson's ratio, R – tensile strength, e – ultimate normal strain.

Uniform composites M, T are homogenized and modelled as linearly elastic – short orthotropic materials, described by the following material constants:

a) elasticity constants:

$$E_1, E_2, E_3, \nu_{12}, \nu_{23}, \nu_{31}, G_{12}, G_{23}, G_{31} \tag{1}$$

b) ultimate strengths:

$$X_t, X_c, Y_t, Y_c, Z_t, Z_c, S_{12}, S_{23}, S_{31} \tag{2}$$

c) ultimate strains:

$$e_{1t}, e_{1c}, e_{2t}, e_{2c}, e_{3t}, e_{3c}, g_{12}, g_{23}, g_{31} \tag{3}$$

with:

$$E_1 = 0.5(E_{1t} + E_{1c}),\ \ E_2 = E_1\ ,\ \ E_3 = E_{3c} \tag{4}$$

$$\nu_{12} = 0.5(\nu_{12t} + \nu_{12c}),\ \ \nu_{13} = \nu_{13c}\quad \nu_{23} = \nu_{13},\ \ \nu_{31} = \nu_{13}E_3/E_1 \tag{5}$$

$$G_{23} = G_{13}\ ,\ \ G_{31} = G_{13} \tag{6}$$

$$Y_t = X_t\ ,\ \ Y_c = X_c\ ,\ \ Z_t = R\ ,\ \ S_{23} = S_{13}\ ,\ \ S_{31} = S_{13} \tag{7}$$

$$e_{2t} = e_{1t}\ ,\ \ e_{2c} = e_{1c}\ ,\ \ e_{3t} = e \tag{8}$$

$$g_{23} = g_{13}\ ,\ \ g_{31} = g_{13} \tag{9}$$

The average values of the material constants of uniform laminates M and T, based on five specimens in each test, are set up in Tab. 1. The standard deviations did not exceed 5% of the respective average values.

Tab. 1. The material constants of uniform composites M and T (the average values)

Parameter	M	T
E_1 [MPa]	8250	16550
E_2 [MPa]	8250	16550
E_3 [MPa]	4150	5000
ν_{12} [–]	0.390	0.155
ν_{23} [–]	0.235	0.234
ν_{31} [–]	0.118	0.0707
G_{12} [MPa]	3040	2300
G_{23} [MPa]	3100	2400
G_{31} [MPa]	3100	2400
X_t [MPa]	95.7	269
X_c [MPa]	216	202
Y_t [MPa]	95.7	269
Y_c [MPa]	216	202
Z_t [MPa]	70	70
Z_c [MPa]	231	344
S_{12} [MPa]	91.0	32.6
S_{23} [MPa]	35.9	22.5
S_{31} [MPa]	35.9	22.5
e_{1t} [–]	0.021	0.021
e_{1c} [–]	0.031	0.011
e_{2t} [–]	0.021	0.021
e_{2c} [–]	0.031	0.011
e_{3t} [–]	0.017	0.020
e_{3c} [–]	0.061	0.100
g_{12} [–]	0.043	0.050
g_{23} [–]	0.040	0.045
g_{31} [–]	0.040	0.045
μ [1)] [–]	0.29	0.29

1) Coulomb friction coefficient for steel–composite pair determined using the inclined plane method

The 3-point bending test, performed according to standard PN-EN ISO 14125:2001, is depicted in Fig. 1. The beam specimens had overall dimensions 80×15×6.1 mm. The initial theoretical span length of beam specimens equals to 64 mm. The central cylindrical mandrel and cylindrical supporting mandrels, of radius r = 5 mm, were parallel to each other. The vertical velocity of the test machine traverse was equal 1 mm/min. There were registered the vertical pressure force F of the central mandrel and the vertical displacement s of the traverse, with sampling frequency 10 Hz. Five specimens were examined.

Bending test examination for the selected specimen is illustrated in Fig. 2, whereas the test results for five specimens are presented in Fig. 3. Good conformity, both qualitative and quantitative, of quasi-linear relationship $F – s$ in the elastic range is observed in Fig. 3 for the examined samples. The failure process started from the bottom lamina M working in tension first of all, which has its tensile strength smaller twice compared to its compressive strength (Tab. 1, Fig. 2). Next, subsequent laminas fractured in correlation with respective strengths. Thus, progressive – catastrophic damage process is observed. Conformity of the $F – s$ curves in the failure zone for five examined specimens is assessed as good from the qualitative point of view. The deviations result from the manufacturing technology first of all, which leads to non-uniform laminas in microscale (spread in ultimate strengths and strains).

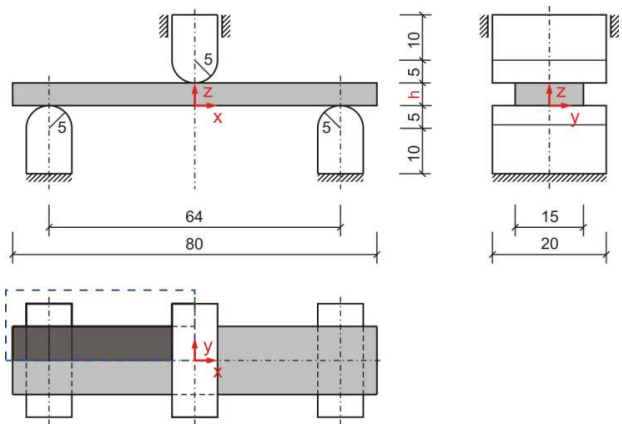

Fig. 1. A scheme of the 3-point bending test of layered composites (a bisymmetric system) with the marked quarter selected for numerical modelling (h=6.1 mm), according to PN-EN ISO 14125:2001

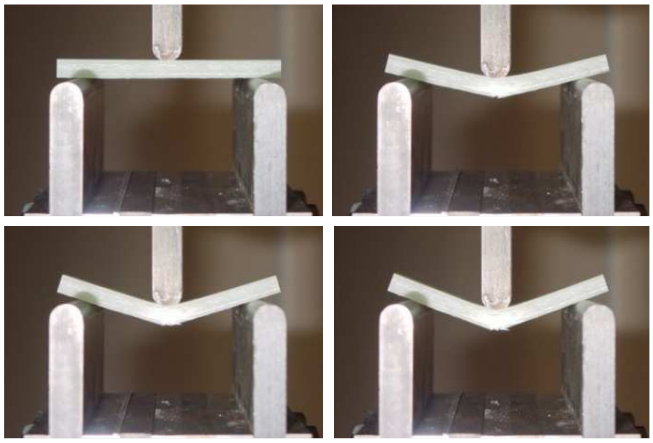

Fig. 2. Photos illustrating the 3-point bending test of the selected MT beam specimen

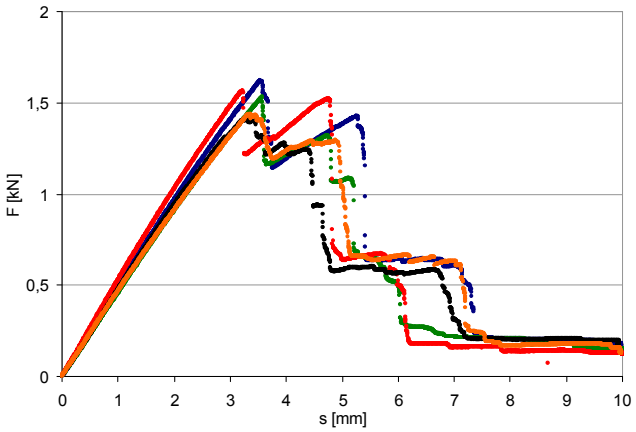

Fig. 3. The $F – s$ diagrams for five examined MT beam specimens in the 3-point bending test

Within the framework of the bending test the material constants characteristic for the 3-point beam bending test have been determined using the classic dependences from standard PN-EN ISO 14125:2001. The ultimate normal stress at bending is calculated for the bottom fibres at the midspan, according to the formula:

$$\sigma_f = \frac{3F_{\max}L}{2bh^2} \tag{10}$$

where: σ_f [MPa] – ultimate normal stress at bending, $F_{\max}$ [N] – load capacity, *L* [mm] – theoretical span length, *h* [mm] – specimen thickness, *b* [mm] – specimen width.

The ultimate normal strain for the bottom fibres is calculated from the formula:

$$e_f = \frac{6 s_{\max} h}{L^2} \tag{11}$$

where: $s_{\max}$ [mm] – deflection corresponding to $F_{\max}$ at the mid-span.

The average values for five specimens amount to:

– the load capacity and the ultimate normal stress: $F_{\max} = 1.51\ \text{kN}, \sigma_f = 264\ \text{MPa}$;
– deflection at the load $F_{\max}$ and the ultimate normal strain at the same conditions: $s_{\max} = 3.43\ \text{mm},\ e_f = 0.03$.

3. NUMERICAL RESEARCH RELATED TO THE MT COMPOSITE BAEM BENDING TEST

Numerical modelling of the 3-point static bending test of the MF composite beam has been conducted using FE code MSC.Marc. The input data have been declared using the following units system: [mm, s, N, K, MPa]. The orthotropy directions 1, 2, 3 for the laminate coincide with the symmetry *x, y, z* axes of the cubicoidal specimen (Fig. 1). Owing to bisymmetry, the FE modelling was limited to a quarter of the system, putting respective boundary conditions. The following assumptions have been adopted:

1. the beam is in static simple bending and shear at bending;
2. the laminas are homogenized and modelled as linearly elastic–short orthotropic materials;
3. each lamina has [0/90] orientation with respect to the beam axis and behaves like an orthotropic material up to short falilure;
4. the central and supporting steel mandrels are modelled as cylindrical rigid surfaces;
5. the central mandrel moves vertically at constant velocity up to 10 mm; at constant geometric increment in the nonlinear process simulation one obtains *ds* = 0.01 mm for 1000 increments;
6. single-side contact and Coulomb friction between steel and composite parts are taken into consideration;
7. the process is physically and geometrically nonlinear (linear elastic–short material, large displacements, small strains).

A discrete model of the system and its components creating respective contact pairs are shown in Fig. 4. The symmetry conditions are reflected by two planes of symmetry defined in the contact options. Taking into consideration the characteristic overall dimensions of laminate beams investigated in the study, a 3D 8-node solid shell element (element type 185 with brick topology), has been chosen, with 24 DOFs (3 translations at each node) and selective reduced integration. This element is based on the second-order laminate theory and is recommended in MSC.Marc system for laminates (2008a, 2008b, 2008c). The element uses the enhanced assumed strain formulation for transverse (through the laminate thickness) normal component and the assumed strain formulation for transverse shear components. These options enable meshing with one layer of finite elements through the laminate thickness (MSC.Marc/Mentat, 2008b).

The stiffness of this element is formed using one integration point in the element plane and three integration points in every lamina (using Simpson's rule). In the case of homogeneous materials five integration points are applied. An additional variationally consistent stiffness term is automatically included to eliminate the hourglass modes. Topology and Gauss points location in Element_185 are depicted in Fig. 5.

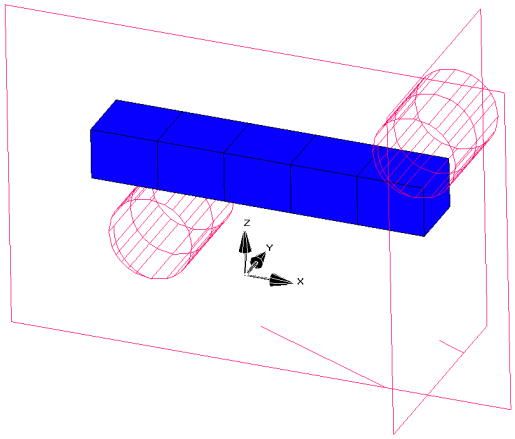

Fig. 4. An FE model of the quarter of the system and components creating contact pairs

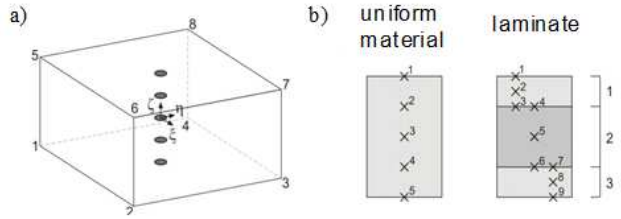

Fig. 5. Element_185 (Solid Shell): a) topology; b) Gauss points (MSC.Marc/Mentat, 2008b)

For comparative purposes finite elements No. 75 and 149 were also tested. Element_75 is a 2D 4-node bilinear thick shell element with 24 DOFs (three translations and three rotations at each node). Element_149 (*Composite Brick Element*) has 8 nodes and corresponds to the orthotropic continuum theory. Laminas are to be parallel to each other. The element is integrated using a numerical scheme based on Gauss quadrature; each lamina contains 4 integration points. The strain-stress relations take into account normal and shear deformations.

The touching contact was tested at 0.05–0.25 mm distance tolerance and 0.95 bias factor. Contact is solved with the direct constraint procedure. The motion of the bodies is tracked, and when contact occurs, direct constraints are placed on the motion using boundary conditions, both kinematic constraints on transformed degrees of freedom and nodal forces. A Coulomb bilinear friction model was used with ultimate stress σ_u=91 MPa.

The preliminary numerical experiments have indicated appropriate failure models. For E-glass mat reinforced homogeneous laminate *Max Strain* failure criterion has been chosen, for which 6 failure indices (FI1–FI6) are calculated at each integration point. The FI values belong to 0–1 interval and are calculated from the following formulas (MSC.Marc/Mentat, 2008b):

$$\begin{aligned}
&\text{FI1} = \left(\frac{\varepsilon_1}{e_{1t}}\right) \text{ for } \varepsilon_1 > 0\,, \quad \text{FI1} = \left(-\frac{\varepsilon_1}{e_{1c}}\right) \text{ for } \varepsilon_1 < 0 \\
&\text{FI2} = \left(\frac{\varepsilon_2}{e_{2t}}\right) \text{ for } \varepsilon_2 > 0\,, \quad \text{FI2} = \left(-\frac{\varepsilon_2}{e_{2c}}\right) \text{ for } \varepsilon_2 < 0 \\
&\text{FI3} = \left(\frac{\varepsilon_3}{e_{3t}}\right) \text{ for } \varepsilon_3 > 0\,, \quad \text{FI3} = \left(-\frac{\varepsilon_3}{e_{3c}}\right) \text{ for } \varepsilon_3 < 0 \\
&\text{FI4} = \left(\frac{\gamma_{12}}{g_{12}}\right)\,, \quad \text{FI5} = \left(\frac{\gamma_{23}}{g_{23}}\right)\,, \quad \text{FI6} = \left(\frac{\gamma_{31}}{g_{31}}\right)
\end{aligned} \tag{12}$$

where: $\varepsilon_1, \varepsilon_2, \varepsilon_3$ – normal strains, $\gamma_{12}, \gamma_{23}, \gamma_{31}$ – shear strains.

For E-glass fabric reinforced homogeneous laminate *Hashin Fabric* failure criterion has been chosen, for which 6 failure indices (FI1–FI6) are calculated at each integration point. These indices reflect the experimentally supported relationships among components of the stress tensor at any point of a T lamina. Indices FI1, FI2 describe material effort with dominant tension/compression of the fibres in direction 1, respectively. Similarly, indices FI3, FI4 describe material effort with dominant tension /compression of the fibres in direction 2, respectively. Indices FI5, FI6 describe material effort with dominant tension /compression of the matrix. The FI values belong to 0-1 interval and are calculated from the following formulas (MSC.Marc/Mentat, 2008b):

$$\begin{aligned}
\mathrm{FI1} &= \left[\left(\frac{\sigma_1}{X_t}\right)^2 + \left(\frac{\sigma_{12}}{S_{12}}\right)^2 + \left(\frac{\sigma_{13}}{S_{13}}\right)^2\right] \text{ for } \sigma_1 > 0 \\
\mathrm{FI2} &= \left[\left(\frac{\sigma_1}{X_c}\right)^2 + \left(\frac{\sigma_{12}}{S_{12}}\right)^2 + \left(\frac{\sigma_{13}}{S_{13}}\right)^2\right] \text{ for } \sigma_1 < 0 \\
\mathrm{FI3} &= \left[\left(\frac{\sigma_2}{Y_t}\right)^2 + \left(\frac{\sigma_{12}}{S_{12}}\right)^2 + \left(\frac{\sigma_{13}}{S_{13}}\right)^2\right] \text{ for } \sigma_2 > 0 \\
\mathrm{FI4} &= \left[\left(\frac{\sigma_2}{Y_c}\right)^2 + \left(\frac{\sigma_{12}}{S_{12}}\right)^2 + \left(\frac{\sigma_{13}}{S_{13}}\right)^2\right] \text{ for } \sigma_2 < 0 \qquad (13) \\
\mathrm{FI5} &= \left[\left(\frac{\sigma_3}{Z_t}\right)^2 + \left(\frac{\sigma_{12}}{S_{12}}\right)^2 + \left(\frac{\sigma_{13}}{S_{13}}\right)^2 + \left(\frac{\sigma_{23}}{S_{23}}\right)^2\right] \text{ for } \sigma_3 > 0 \\
\mathrm{FI6} &= \left[\left(\frac{\sigma_3}{Z_c}\right)^2 + \left(\frac{\sigma_{12}}{S_{12}}\right)^2 + \left(\frac{\sigma_{13}}{S_{13}}\right)^2 + \left(\frac{\sigma_{23}}{S_{23}}\right)^2\right] \text{ for } \sigma_3 < 0
\end{aligned}$$

where: $\sigma_1, \sigma_2, \sigma_3$ – normal stresses, $\sigma_{12}, \sigma_{13}, \sigma_{23}$ – shear stresses.

In both failure models *Progressive Damage* option was used, what results in respective stiffness degradation in laminas. *Selective Gradual Degradation* model that decreases gradually the elasticity constants was selected. The *Full Newton-Raphson* procedure was used to simulate nonlinear processes at the displacement and force convergence criteria with 0.02 tolerance. The time increment is transformed into the geometrical increment (the nominal time of the static process duration is 1 sec).

The simulations were conducted in Department of Mechanics & Applied Computer Science, Military University of Technology, Poland. Each series consumed 5-60 minutes of CPU time. The numerical research has resulted in a set of options/values of the parameters recommended in numerical modelling and simulation of static processes, including progressive failure, in glass-polyester mixed layered composite structures. Tab. 2 gives the recommended values of the parameters related to an adaptive time step, whereas Tab. 3 collects the recommended options/values of the numerical modelling and simulation parameters.

Tab. 2. The recommended values of parameters related to an adaptive time step (MSC.Marc 2008a)

Parameter	Default	Recommended
Initial Fraction of Loadcase Time	0.01	0.001
Minimum Fraction of Loadcase Time	10^{-5}	10^{-6}
Maximum Fraction of Loadcase Time	0.5	0.1
Desired #Recycles / Increment	5	20
Time Step Scale Factor	1.2	1.01

Figs. 7–11 depict diagrams of the central mandrel pressure force *F* vs. the traverse vertical displacement *s*, reflecting selected final numerical tests that constitute the base for determination of the options/values of numerical modelling and simulation parameters, recommended in engineering calculations. The simulated diagrams (in colour) are presented against a background of experimental curves for five specimens (in grey). The simulated curve in red corresponds to the option/values collected in Tab. 3, recommended for modelling and simulation of static processes, including failure, in beam/plate/shell GFRP composite structures.

Tab. 3. The recommended options/values of numerical modelling and simulation parameters

Parameter	Option/value
Element Types	185 (*Solid Shell*)
Element Dimensions	close to laminate thickness
FAILURE	
Failure Criteria	*Hashin Fabric, Max Strain*
Failure	*Progresive Failure*
Stiffness Degradation Method	*Gragual Selective*
Residual Stiffness Factor	0.005
CONTACT	
Support, Mandrel	*Rigid*
Laminate Beam	*Deformable*
Separation Force	0.1
Distance Tolerance	0.15
Bias Factor	0.95
FRICTION	
Type	*Coulomb*
Numerical Model	*Bilinear* (*Displacement*)
Friction Force Tolerance	0.05
Slip Threshold	*Automatic*
ANALYSIS OPTIONS	
Max # Recycles	30
Min # Recycles	2
Iterative Procedure	*Full Newton-Raphson*
Convergence Testing	*Residual and Displacement*
Relative Force Tolerance	0.02
Relative Displacement Tolerance	0.02
Time Step	*Adaptive*
Nonlinear Procedure	*Small Strain* *Assumed Strain* *Large Rotation*
Composite Integration Method	*Full Layer Integration*

The numerical *F–s* diagram obtained for the recommended options/values of numerical modelling and simulation parameters is presented in Fig. 6. Good conformity, both qualitative and quantitative, of the simulation and the experiment is observed in both elastic quasi-linear and catastrophic–progressive failure zones. Values of the ultimate pressure force and corresponding vertical displacement of the pressure mandrel amount to: $F_{\max} = 1.56$ kN, $s_{\max} = 3.21$ mm. The simulated force levels corresponding to catastrophic failure of the subsequent laminas are close to the experimental results.

Fig. 7 compares the numerical diagrams obtained for a 3D 8-node solid shell element (185) and for two other FE types, i.e. an isoparametric 3D 8-node composite brick element (149) and a 2D 4-node 24 DOF bilinear thick shell element (75). Ele-

ment 185 gives the diagram which is very close to the average experimental response.

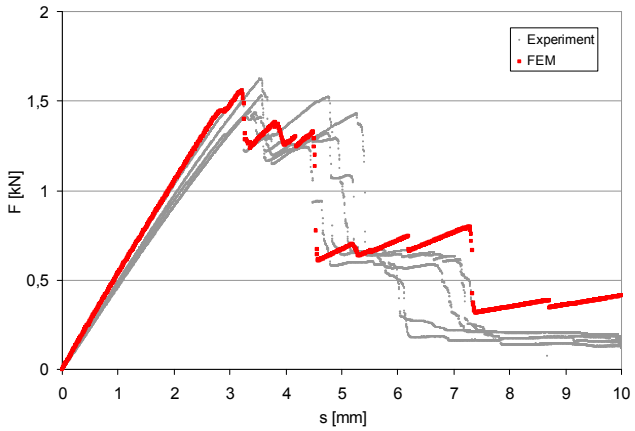

Fig. 6. The simulated *F – s* diagram against a background of the experimental diagrams for five specimens. The most correct numerical solution

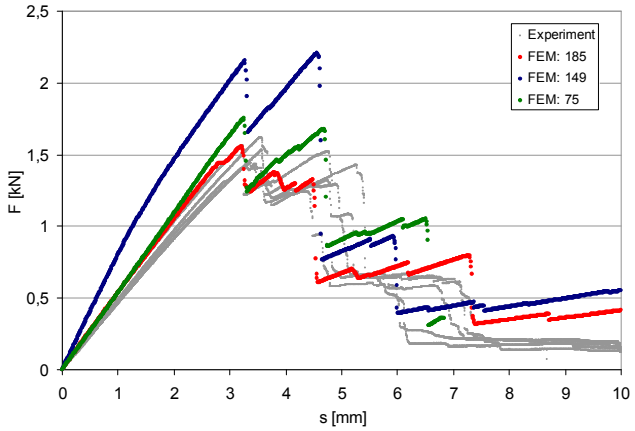

Fig. 7. The simulated curves for selected FE types against a background of the experimental curves

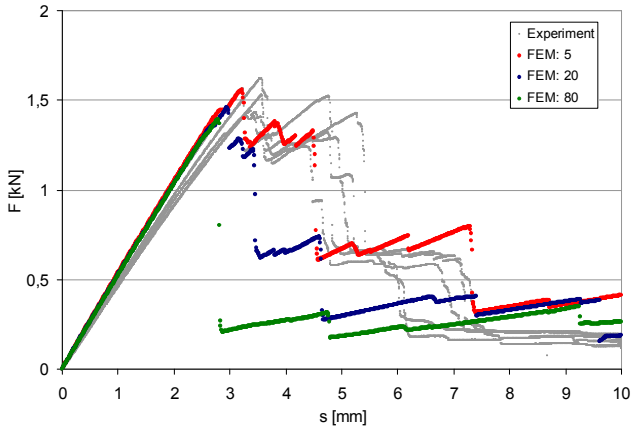

Fig. 8. The simulated curves for selected FE mesh densities against a background of the experimental curves

Fig. 8 presents the *F–s* curves for three FE mesh densities (5, 20, 80 FEs for the quarter of the examined system). Diagrams presented in Fig. 9 reflect the influence of small or large deformations assumption. Fig. 10 shows the results related to testing Residual Stiffness Factor (RSF). It reflects the initial stiffness part below which the laminate stiffness will not be reduced. For RSF=0.005 progressive failure is the most close to reality (smaller values of RSF do not lead to better results). The results reflecting testing a time step (adaptive; 0.001; 0.02) are presented in Fig. 11. The diagrams for an adaptive step and a constant 0.001 mm step are identical.

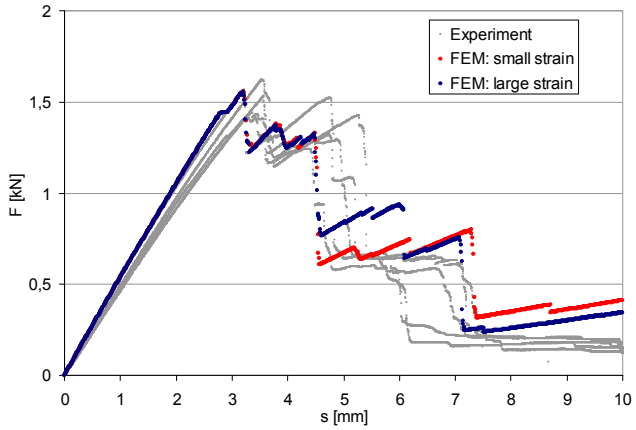

Fig. 9. The simulated curves under small / large strains assumption against a background of the experimental curves

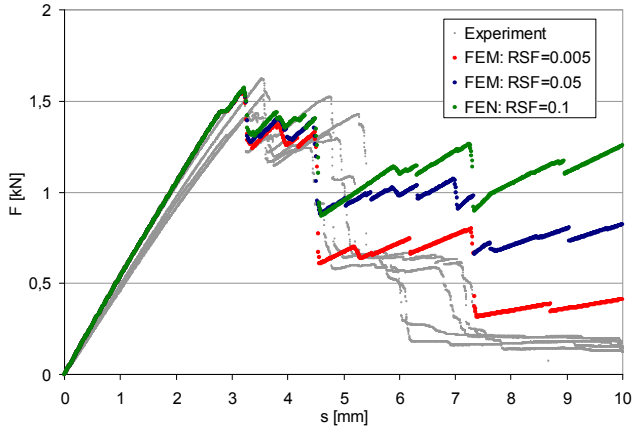

Fig. 10. The simulated curves for selected values of RSF against a background of the experimental curves

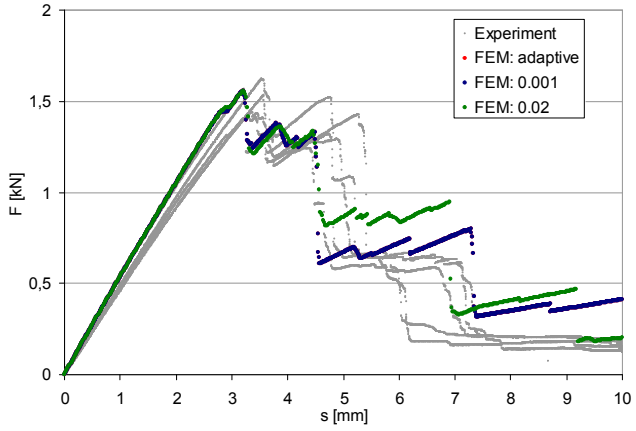

Fig. 11. The simulated curves for selected variants of the displacement increment against a background of the experimental curves

It has been proved that the overall dimensions of FEs in the *xy* plane (the laminate plane) should be close to the laminate thickness, the small strain assumption is correct for linearly elastic–short materials with progressive stiffness degradation beyond the ultimate strains, and an adaptive time step is recommended in the simulations.

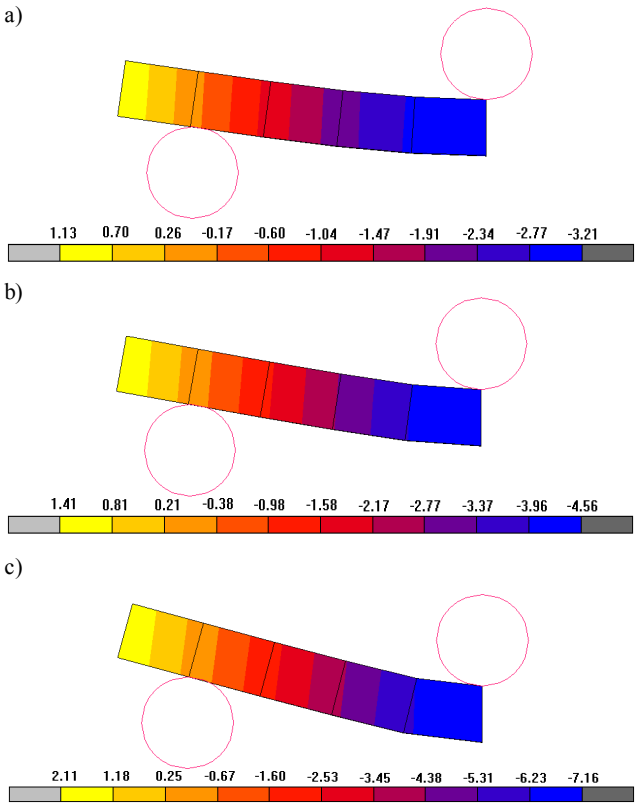

Fig. 12. Vertical displacement contours of the beam quarter (a side view) for selected punch displacements: a) 3.21 mm (the state closely before failure initiation); b) 4.56 mm; c) 7.16 mm

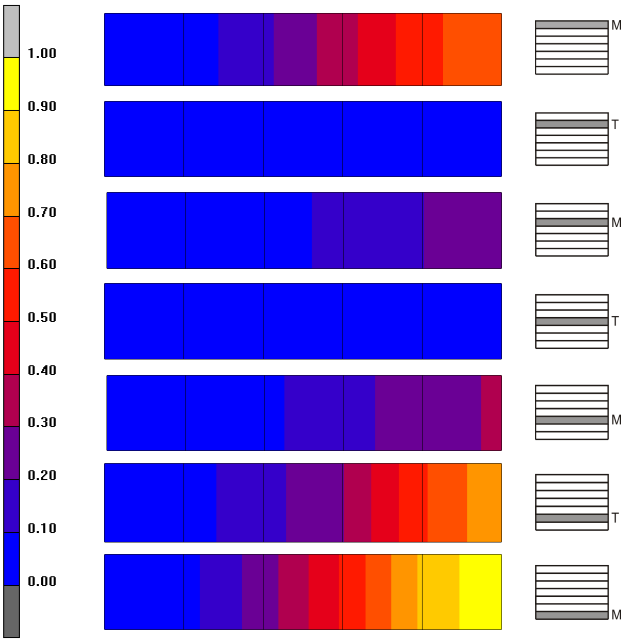

Fig. 13. Contours of the 1st failure index closely before progressive damage initiation in subsequent laminas (a top view onto the beam quarter)

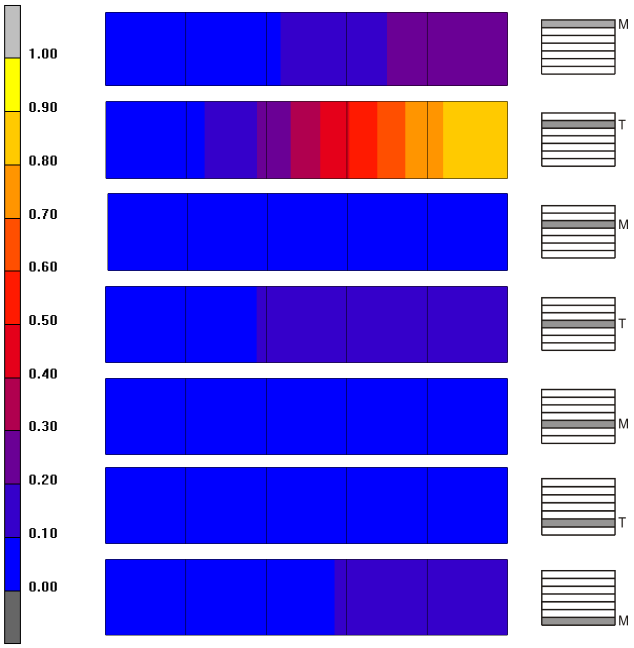

Fig. 14. Contours of the 2nd failure index closely before progressive damage initiation in subsequent laminas (a top view onto the beam quarter)

Simulations of processes using advanced CAE systems have practically unlimited possibilities in tracking the process at any point of the system. This is the basic advantage of numerical research over experimental research. Representative results illustrating simulation of the 3-point bending test for an MT composite beam are presented in Figs. 12–14.

Fig. 12 shows vertical displacement contours of the beam quarter (a side view) for the selected displacements of the punch. These contours are very close to respective experimental displacements (not presented in this study) of the bent specimens.

Failure indices defined in Eqns. (12, 13) are commonly used as measures of material effort in subsequent laminas. Contours of the 1st and 2nd failure indices in subsequent laminas before catastrophic–progressive damage initiation, corresponding to different failure mechanisms for M and T laminas, are collected in Figs. 13 and 14. As observed in the experimental tests, destruction of the MT laminate beam is mainly determined by longitudinal normal strains in M-laminas and by longitudinal normal stresses in T-laminas.

4. FINAL CONCLUSIONS

The study develops FE modelling and simulation of static processes, including progressive failure, in beam/plate/shell structures made of GFRP mixed laminates, using FE code MSC.Marc. The standard 3-point bending test of a GFRP mixed laminate beam has been conducted experimentally and numerically. The following extended numerical tests have been performed:

1. tests on selected finite elements allowable in MSC.Marc system for modelling of laminates;
2. tests on mesh density;
3. tests on strain quantity;
4. tests on the residual stiffness factor;
5. tests on a time step.

Based on these tests, a set of options/values of the numerical modelling and simulation parameters, recommended in engineering

calculations, has been determined. The experimental verification of numerical modelling and simulation of the bending test performed on GFRP laminate beams is positive in both the quasi-linear and the catastrophic – progressive failure zones.

REFERENCES

1. ASTM D5379 / D5379M - 98 (1998), *Standard Test Method for Shear Properties of Composite Materials by the V-Natched Beam Method*.
2. *Covering Systems – Technical Concept* (2006), C.F. Maier Europlast GmbH & Co KG, Königsbronn, Germany.
3. *Product Catalogue* (2010), P.T. Glaplast, Kielce (in Polish).
4. LS-DYNA (2009), *Keyword User's Manual*, Version 971/ Release 4 Beta, LSTC, Livermore, CA, USA.
5. Marc 2008 r1 (2008), *User's Guide*, MSC.Software Co., Santa Ana, CA, USA.
6. Marc 2008 r1 (2008), *Theory and User Information*, MSC.Software Co., Vol. A, Santa Ana, CA, USA.
7. Marc 2008 r1 (2008), *Element Library*, MSC. Software Co., Vol. B, Santa Ana, CA, USA.
8. PN-EN ISO 14129 (1997), Fibre-reinforced structural composites. Determination of shear strain and stress, shear modulus and strength at tension at angle ±45° (in Polish).
9. PN-EN ISO 527 (2000), Plastics. Deterniation of mechanical properties at static tension. Test conditions for isotropic/orthotropic fibre-reinforced polymer-matrix composites (in Polish).
10. PN-EN ISO 14125 (2001), Fibre-reinforced structural composites. Determination of properties at bending (in Polish).
11. PN-EN ISO 14130 (2001), Fibre-reinforced structural composites. Determination of nominal interlaminar shear strength using the short beam method (in Polish).
12. PN-EN ISO 14126 (2002), Fibre-reinforced structural composites. Determination of properties at in-plane compression (in Polish).
13. **Vacĭk J., Lašovă V., Kosnar M., Janda P., Kottner R.** (2010), Selection of optimum type FEM model for hybrid composite structure, *Advanced Engineering*, 4.
14. **Zemčĭk R., Laš V., Kroupa T., Purš H.** (2011), *Identification of material characteristics of sandwich panels*, University of West Bohemia in Pilsen, Czech Republik.
15. *Polyester resins* (2008), Engineers' Handbook, Organika-Sarzyna Chemical Plant (in Polish).

The study has been supported by National Centre of Science, Poland as a part of a research project No N506 1228 40, realized in the period 2011-2013. This support is gratefully acknowledged.